where r_0 is the distance from the body axis to the interface, t denotes dimensionless time, and F_x deceleration force. The simplified form of the energy equation (3) is obtained by approximating the convection terms by their limiting form, $v_\infty(\partial T/\partial y)$, for large y where convection is important; near the interface, conduction is assumed to be dominant.

The essential unsteady character of the problem can be noted from the energy equation; without the unsteady effects the temperature could not be bounded at infinity if liquid accumulated ($v_\infty > 0$) at some position. Careful examination of the pressure, shear, and deceleration forces for bodies whose surfaces become parallel to the flight direction shows that after some position on the body the deceleration force becomes uniform and dominates all the other forces. The liquid layer everywhere downstream of this position behaves like a heated semi-infinite slab that is characterized by unsteady effects. These considerations mark the first important deviation from existing work on this problem.

Two parameters characterize the problem. The one in the last term of the momentum equation (2) is essentially the inverse of a Froude number and represents the ratio of deceleration and pressure (or viscous) forces; deceleration effects become significant when this parameter is not small. The other parameter, which appears in the energy equation (3), represents the characteristics of the particular liquid and gives the relative influence of convection and conduction.

Liquid layer outer-boundary conditions are obtained from the gas boundary-layer characteristics of Cohen and Reshotko.[4] The body shape [see Fig. 3(a)] is thus limited to the class for which that analysis pertains. The correct interface temperature T_i is selected to give a consistent energy balance between the gas and liquid layers; the velocity components and shears are also matched. Boundary conditions for the liquid layer thus are: $v = -v_0$, $\partial u/\partial y = (R/h)(\tau_i/P_m)$ at the interface ($y = 0$), and $T = 0$, $u = 0$ at the solid surface ($y = \infty$), where τ_i denotes the shear at the interface. Initial conditions specified are $u = v = T = 0$ at $t = 0$. In the calculated example, a first approximation to T_i is used; viz., T_i = const. Although not investigated, we assume that improvements by iteration are possible and ignore this herein so that the other effects can be most simply shown.

Taking the viscosity-temperature relation to be $\mu = \mu_i \exp [b(x)y]$, we can write the solutions explicitly as

$$u = -(e^{-by}/b)[fy + (f/b) + \bar{\tau}_i] \qquad (4)$$

$$\frac{T}{T_i} = \frac{1}{2}\left[e^{\eta} \operatorname{erfc}\left(\frac{Y+Z}{2}\right) + \operatorname{erfc}\left(\frac{Y-Z}{2}\right)\right] \qquad (5)$$

where

$$\bar{\tau}_i = (R/h)(\tau_i/P_m), \qquad \eta = Pr\ Re(h/R)^2 v_\infty y,$$
$$Y = y/\sqrt{t}, \qquad Z = Pr\ Re(h/R)^2 v_\infty \sqrt{t}$$

At each position x along the body an iteration procedure based on matching the assumed viscosity-temperature law with the actual one for Pyrex[1] at two points is used to determine $b(x)$ and $v_\infty(x)$.

The liquid layer development with no deceleration can be seen in Fig. 1. Negative values of v_∞ indicate a thinning of the liquid layer. Thus, liquid flows away from the stagnation region and tends to accumulate downstream because the shear and pressure decrease. At some later time the thicker layer results in a greater pressure force, and the liquid is moved rearward in a wavelike pattern. In proceeding downstream from the stagnation region with a deceleration force, however, we found that after some time our calculation procedure failed at some point. It was felt that, among other reasons, this occurred because the forward integration could in no way be influenced by upstream flow due to the deceleration force. Accordingly, asymptotic (in x) forms of the basic equations were integrated by the same procedure starting at the rear of the body. The effect of the deceleration force (for $\rho F_x R/P_m = -0.1$) can be seen in Fig. 2. The liquid no longer continues downstream but accumulates at some point on the body. The inhibition of downstream liquid flow results in more effective heat shielding by the layer. It is noteworthy that fortuitously v_∞ computed from the front and the rear for 1.45 sec. match smoothly. Representative profiles at different body stations for this case are shown in Fig. 3. Flow reversal and upstream flow at the back end due to the body force are clearly evident from the velocity distributions. Although the temperature profiles look quite similar at this relatively short time, their slopes at the interface indicate relatively higher heat transfer into the layer in the stagnation region ($\xi = 0$) with the lowest heat transfer at the position of maximum $v_\infty(\xi = 0.6)$.

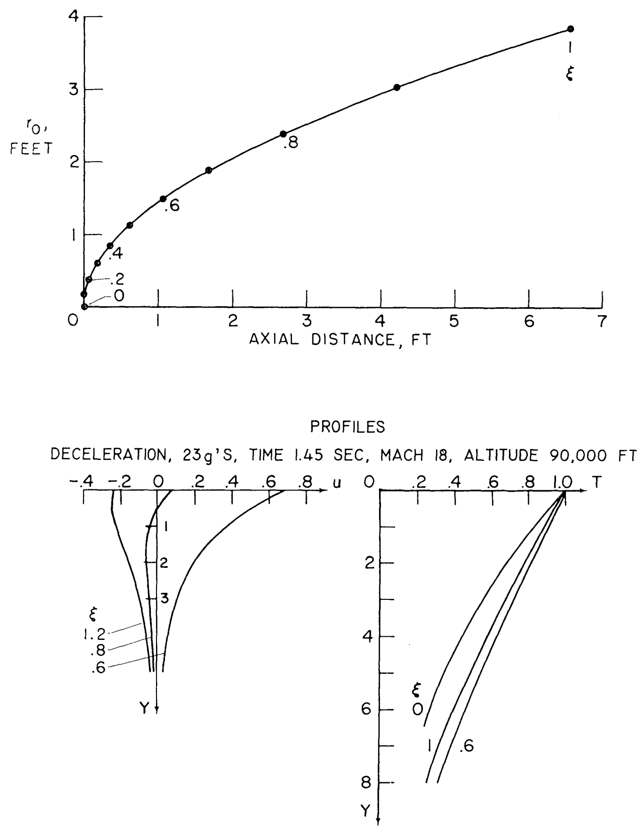

FIG. 3. (a) *Top:* Body shape. (b) *Bottom left:* Velocity. (c) *Bottom right:* Temperature.

References

[1] Sutton, G. W., *The Hydrodynamics and Heat Conduction of a Melting Surface*, Journal of the Aeronautical Sciences, Vol. 25, No. 1, pp. 29–32, January, 1958.

[2] Tellep, D. M., *The Effect of Vehicle Deceleration on a Melting Surface*, Lockheed Missiles and Space Division, Tech. Rept. LMSD-48381, January, 1959.

[3] Fanucci, J. B., and Lew, H. G., *Effect of Mass Transfer and Body Forces on Two Phase Boundary Layers*, General Electric Co., Tech. Inf. Series, Res. Memo. No. 35, April, 1959.

[4] Cohen, C. B., and Reshotko, E., *Similar Solutions for the Laminar Compressible Boundary Layer with Heat Transfer and Pressure Gradient*, NACA Rep. 1293, 1956. (Supersedes NACA TN 3325.)

Tangent-Modulus Column Theory

George Gerard
Associate Director of Research, College of Engineering, New York University
March 23, 1960

Symbols

E = elastic modulus
E_r = reduced modulus
E_t = tangent modulus

$\bar{E}$ = generalized inelastic modulus
I = moment of inertia
L = length
M_e = external bending moment
M_i = internal bending resistance
P = axial compressive load
w = lateral deflection
$\bar{w}$ = initial lateral imperfection
ρ = radius of gyration
σ_a = axial compressive stress
σ_{cr} = compressive buckling stress

Introduction

Experimental results on aluminum-alloy columns led Shanley[1] to re-examine the basic assumptions of inelastic column theory in a now classic paper published in 1947. He concluded that if axial straining and bending proceeded simultaneously at buckling, no strain reversal would occur and, therefore, the tangent modulus is the correct effective modulus for inelastic buckling of a perfect column. Shanley's analysis of an idealized type of inelastic column indicated that a continuous spectrum of possible bent configurations exists for which the lateral deflections increase from zero at the tangent-modulus stress to infinity at the reduced-modulus stress. Thus the tangent-modulus stress is the lowest value at which a bent configuration becomes stable and, therefore, can be considered as the buckling stress.

In commenting on Shanley's contribution, von Kármán[1] indicated that the reduced modulus is correct when the stability analysis is based on the requirement that the axial load remain fixed at the exchange of equilibrium configurations. He contended that because of the nonreversible character of inelasticity, it is necessary to revise the definition of the stability limit. Thus, for inelastic buckling, we should seek"... the smallest value of the axial load at which bifurcation of the equilibrium positions can occur, regardless of whether or not the transition to the bent position requires an increase of the axial load." From this definition, the tangent-modulus buckling stress originally proposed by Engesser is the correct solution.

The analysis presented in this paper utilizes Shanley's concept that axial straining and bending proceed simultaneously without strain reversal in the development of tangent modulus theory. However, it is not assumed that this concept applies to a *perfect* inelastic column, nor is it required that the definition of the stability limit be revised for inelastic buckling. Instead, the theory of an *imperfect* inelastic column (imperfect in a geometric sense) is developed in which case the assumption that axial straining and bending proceed simultaneously without strain reversal is completely rational.

Analysis of Column Types

Since the pertinent differential equations involve equilibrium of bending moments, we shall be particularly interested in the external bending moment, M_e, and the internal bending resistance, M_i for the four column types: perfect and imperfect elastic columns, perfect and imperfect inelastic columns. Only infinitesimal lateral deflections are considered because we are concerned here with the buckling behavior.

The usual relations for the bending moments are listed in Table 1 where w is the lateral deflection of the column always measured from the initial position, $\bar{w}$. For perfect columns, of course, $\bar{w} = 0$.

Although the values of M_i given in Table 1 are familiar, it should be noted that for the *perfect* inelastic column, E_r is based on the assumption that bending starts at buckling under a fixed axial load and, therefore, a strain reversal occurs. On the other hand, for the *imperfect* inelastic column, axial loading and bending proceed simultaneously from the start due to the geometric imperfection. Hence, the tangent modulus is appropriate in this case.

In all cases, we seek a solution of the equilibrium equation

$$(d^2w/dx^2) + (\sigma/\bar{E}\rho^2)(w + \bar{w}) = 0 \quad (1)$$

Table 1

Column Type	M_e	M_i	σ_{cr}
perfect elastic	Pw	$-EI(d^2w/dx^2)$	$\pi^2E\rho^2/L^2$
imperfect elastic	$P(w + \bar{w})$	$-EI(d^2w/dx^2)$	$\pi^2E\rho^2/L^2$
perfect inelastic	Pw	$-E_rI(d^2w/dx^2)$	$\pi^2E_r\rho^2/L^2$
imperfect inelastic	$P(w + \bar{w})$	$-E_tI(d^2w/dx^2)$	$\pi^2E_t\rho^2/L^2$

For perfect columns, $\bar{w} = 0$, and therefore the solution is determined for characteristic values of σ as given in Table 1. For imperfect columns, the initial geometric imperfection can be conveniently represented by

$$\bar{w} = \sum_{n=1}^{\infty} \bar{w}_n \sin(n\pi x/L) \quad (2)$$

Similarly, the lateral deflection for a simply supported column

$$w = \sum_{n=1}^{\infty} w_n \sin(n\pi x/L) \quad (3)$$

By carrying out the analysis for the imperfect inelastic column, it can be determined that

$$w_n/\bar{w}_n = \left[\frac{(n^2\pi^2E_t\rho^2/L^2)}{\sigma_a} - 1\right]^{-1} \quad (n = 1, 2, 3 \ldots) \quad (4)$$

As the axial compressive stress σ_a approaches $\pi^2E_t\rho^2/L^2$, which can be identified as the limiting value of axial compressive stress, σ_{cr}, for this case, the $n = 1$ term dominates Eq. (3). In addition as σ_a approaches σ_{cr}, the tangent modulus becomes substantially constant.

Thus, in the region of buckling, the lateral deflection at the center of the column is approximated by

$$w/\bar{w}_1 = [(\sigma_{cr}/\sigma_a) - 1]^{-1} \quad (5)$$

where

$$\sigma_{cr} = \pi^2E_t\rho^2/L^2 \quad (6)$$

For the imperfect elastic column, $E_t = E$ and Eq. (6) reduces to the familiar Euler equation as indicated in Table 1.

Comparison of Solutions

At this point, it is most interesting to compare the solutions for perfect and imperfect columns. In the *elastic* case, the limiting axial compressive stress for a column containing small initial geometrical imperfections is identical with the buckling stress of a corresponding perfect column as shown in Table 1.

In comparing the *inelastic* solutions given in Table 1, however, the buckling stress of a perfect column is always higher than the limiting axial compressive stress of an imperfect column, Eq. (6). Since the latter represents the buckling stress of a column with vanishingly small initial imperfections, the tangent-modulus buckling stress can be considered as the correct theoretical inelastic generalization of the Euler stress. On the basis of experimental evidence, it has so been considered for a long time.

Reference

[1] Shanley, F. R., *Inelastic Column Theory*, Journal of the Aeronautical Sciences, Vol. 14, No. 5, pp. 251–267, May, 1947. (Also discussion by T. von Kármán.)

Reynolds-Analogy Parameter for the Laminar Boundary Layer With Blowing, Pr = 3/4

C. R. Faulders
Aero-Space Laboratories, Missile Division, North American Aviation, Inc., Downey, Calif.
March 22, 1960

Symbols

h = enthalpy
k = thermal conductivity